

The DIAP1 RING finger mediates ubiquitination of Dronc and is indispensable for regulating apoptosis

Rebecca Wilson*§, Lakshmi Goyal†§, Mark Ditzel*§, Anna Zachariou*, David A. Baker‡, Julie Agapite†, Hermann Steller† and Pascal Meier*#

*The Breakthrough Toby Robins Breast Cancer Research Centre, Institute of Cancer Research, Chester Beatty Laboratories, Fulham Road, London SW3 6JB, UK

†Howard Hughes Medical Institute, Rockefeller University, New York, NY 10021, USA

‡Institute of Reproductive and Developmental Biology, Faculty of Medicine, Imperial College of Science & Technology, London W12 0NN, UK

§These authors contributed equally to this work

#e-mail: pmeier@icr.ac.uk

Published online: 14 May 2002, DOI: 10.1038/ncb799



Members of the Inhibitor of Apoptosis Protein (IAP) family block activation of the intrinsic cell death machinery by binding to and neutralizing the activity of pro-apoptotic caspases. In *Drosophila melanogaster*, the pro-apoptotic proteins Reaper (Rpr), Grim and Hid (head involution defective) all induce cell death by antagonizing the anti-apoptotic activity of *Drosophila* IAP1 (DIAP1), thereby liberating caspases. Here, we show that *in vivo*, the RING finger of DIAP1 is essential for the regulation of apoptosis induced by Rpr, Hid and Dronc. Furthermore, we show that the RING finger of DIAP1 promotes the ubiquitination of both itself and of Dronc. Disruption of the DIAP1 RING finger does not inhibit its binding to Rpr, Hid or Dronc, but completely abrogates ubiquitination of Dronc. Our data suggest that IAPs suppress apoptosis by binding to and targeting caspases for ubiquitination.

Programmed cell death, or apoptosis, is central to the processes of animal development¹. Apoptosis is executed by a set of highly specific cysteine proteases, called caspases². Once activated, initiator caspases cleave and activate 'downstream' or 'effector' caspases³. These effector caspases cleave various structural and regulatory proteins, resulting in the orchestrated collapse of the cell, a feature characteristic of apoptosis⁴. Activation of caspases is tightly regulated by members of the IAP family^{5,6}. In *Drosophila*, loss-of-function mutations in the gene *thread* (*th*), which encodes DIAP1, results in early embryonic death through illicit activation of apoptosis^{7–9}. The current model suggests that IAPs block apoptosis by directly binding to caspases, thereby preventing caspases access to their substrates¹⁰. It seems that in *Drosophila*, Rpr, Grim and Hid induce cell death by binding to DIAP1, thereby liberating caspases^{7,9}. Although it is clear that direct binding of DIAP1 to Dronc is essential for the regulation of Dronc *in vivo*, little is known about the molecular mechanisms through which DIAP1 blocks Dronc activation. In addition to the baculovirus IAP repeat (BIR), some IAPs also contain a carboxy-terminal RING finger; a small zinc-binding domain found in many functionally distinct proteins. Recent results suggest that proteins with RING finger domains function as E3 ubiquitin protein ligases¹¹.

In this study we elucidate the function of the DIAP1 RING finger domain in apoptosis. It has been demonstrated that ectopic expression of Rpr and Hid in the developing retina induces excessive cell death, resulting in a rough and reduced eye^{12–14}. In a genetic

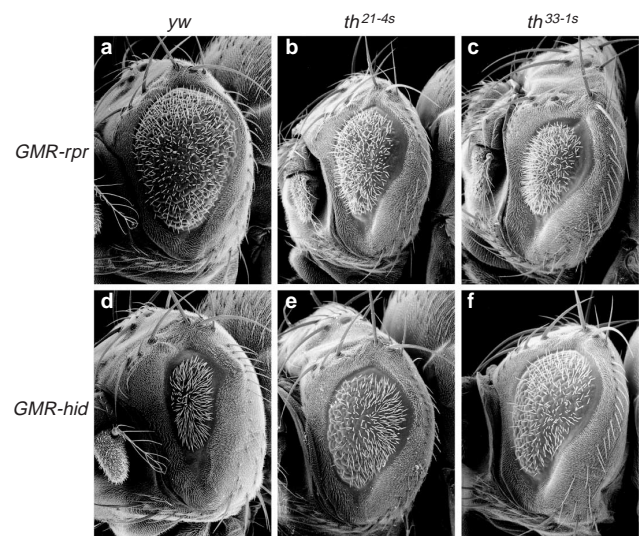


Figure 1 Mutations affecting the RING finger of DIAP1 modify *rpr*- and *hid*-induced cell death in the fly eye. **a–c**, Scanning electron microscope images of GMR-*rpr*-induced eye phenotypes. Targeted expression of Rpr in the developing eye results in a small eye phenotype (**a**; GMR-*rpr*/+) that is significantly enhanced in flies with either a point mutation in the RING finger of DIAP1, *th*^{21-4s} (**b**; GMR-*rpr*/*th*^{21-4s}), or a deletion of the entire RING finger, *th*^{33-1s} (**c**; GMR-*rpr*/*th*^{33-1s}). **d–f**, Scanning electron microscope images of GMR-*hid*-induced eye phenotypes. Unmodified Hid eye phenotype (**d**; GMR-*hid*/+). *diap1* RING finger mutations, *th*^{21-4s} (**e**; GMR-*hid*/*th*^{21-4s}) and *th*^{33-1s} (**f**; GMR-*hid*/*th*^{33-1s}) suppress the Hid eye phenotype.

screen performed to isolate modifiers of this eye phenotype, three classes of *diap1* alleles were obtained (J.A., K. McCall and H.S., unpublished observations)¹⁵ (Fig. 2a). Characterization of *diap1* gain-of-function alleles (class I) and loss-of-function alleles (class III) have been previously reported^{8,9}. Class II *diap1* mutants (Fig. 2a and Supplementary Information, Table SI) were enhancers of *rpr*-induced cell death in the eye but suppressors of *hid*-induced eye ablation (Fig. 1). Molecular analysis mapped the class II mutations to the RING finger domain of DIAP1 (Fig. 2a and Supplementary Information, Table SI). Consistent with the fly data (Fig. 1), we

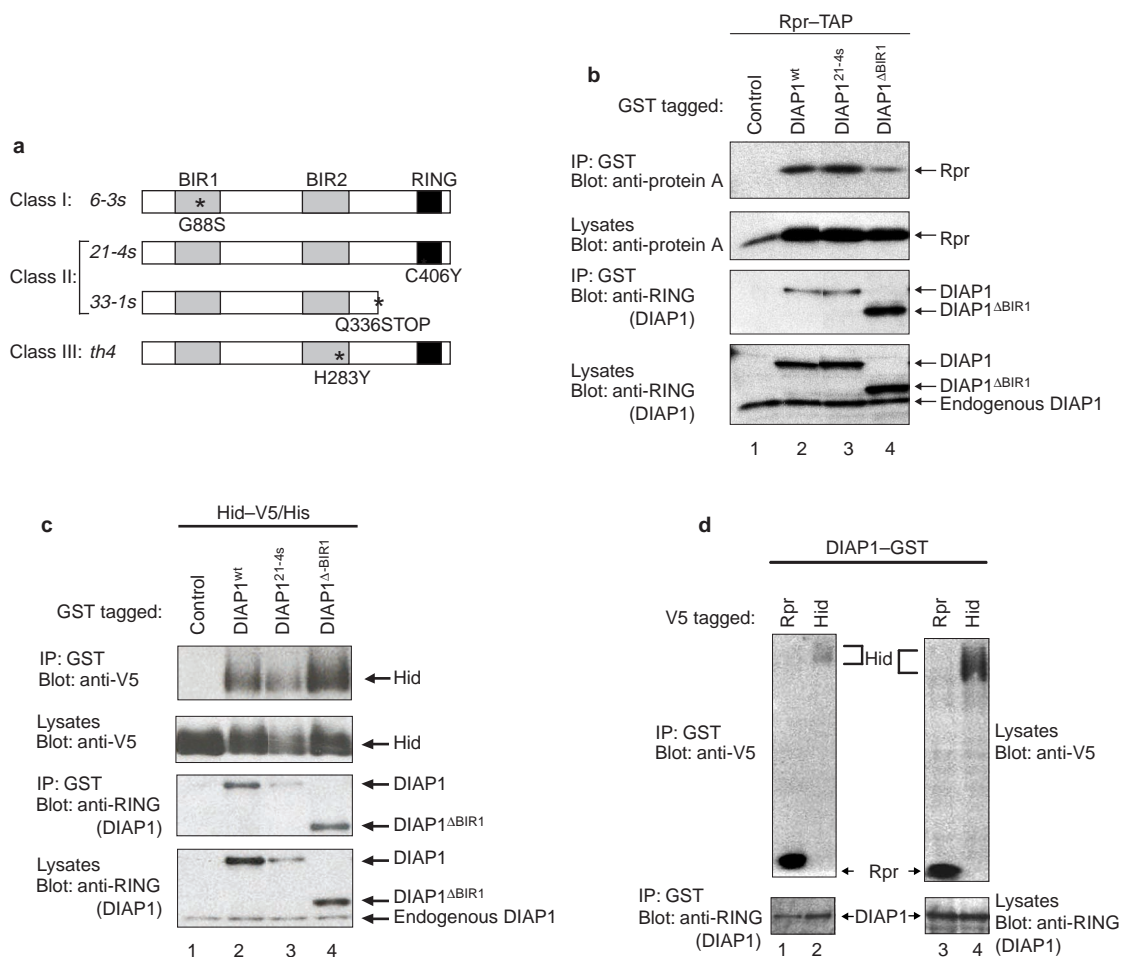


Figure 2 RING finger mutations do not affect the binding of Rpr and Hid to DIAP1. **a**, A schematic representation of three classes of *diap1* mutants characterized in this study. **b**, Rpr binds with equal efficiency to wild-type or mutant DIAP1. Copurification of Rpr with DIAP1 from cellular extracts is shown. S2 cells were transiently transfected with the indicated combinations of constructs, encoding TAP-tagged Rpr and GST-tagged wild-type or mutant DIAP1. A DIAP1 mutant lacking the first BIR domain (Δ BIR1) was also included in this study. DIAP1 was purified from cell lysates using glutathione beads and associated Rpr was detected by immunoblot analysis using antibodies directed against protein A present in the TAP tag fused to Rpr (top). Expression of TAP-tagged Rpr and GST-tagged DIAP1 in S2 cells was confirmed by immunoblotting with the indicated antibodies (second and fourth panels). Effective DIAP1 purification was determined by immunoblotting the GST-DIAP1-containing eluate with an anti-DIAP1 RING finger antibody (third panel). **c**, The binding of Hid to DIAP1 is not affected by a RING finger mutation. Copurification of Hid with DIAP1 from cellular extracts are shown. S2 cells were

cotransfected with the indicated constructs, encoding V5-tagged Hid and GST-tagged wild-type or mutant DIAP1. DIAP1 was purified as described in **a** and the presence of copurified Hid was examined by immunoblotting with an anti-V5 antibody (top). Expression of V5-tagged Hid and GST-tagged DIAP1 was confirmed by immunoblotting with the indicated antibodies (second and fourth panels). DIAP1 purification was determined as in **b** (third panel). **d**, Hid has a significantly lower binding affinity for DIAP1 than Rpr. Copurification of Rpr and Hid with DIAP1 from cellular extracts are shown. S2 cells were cotransfected with the indicated constructs, encoding V5-tagged Rpr and Hid and GST-tagged wild-type DIAP1. DIAP1 was purified as described in **b** and the presence of copurified Rpr and Hid was examined by immunoblotting with an anti-V5 antibody (top left panel, lanes 1 and 2). Expression of V5-tagged Rpr and Hid (top right panel, lanes 3 and 4) and GST-tagged DIAP1 (bottom right panel, lanes 3 and 4) was confirmed by immunoblotting with the indicated antibodies. DIAP1 purification was determined as in **b** (bottom left panel, lanes 1 and 2).

found that in a cell death assay using cultured *Drosophila* S2 cells, mutation of the DIAP1 RING finger (class II, *th*^{21-4s} and *th*^{33-1s}) failed to rescue Rpr-induced cell death but readily alleviated Hid-mediated killing (Supplementary Information, Fig. S1). Thus, mutation of the RING finger of DIAP1 results in a failure to regulate apoptosis induced by ectopic expression of Rpr and Hid.

Because Rpr and Hid induce cell death by binding to DIAP1 (refs 7,9), we examined DIAP1 RING mutant proteins for their ability to bind to Rpr and Hid. To this end, we co-expressed DIAP1 RING finger mutants fused to glutathione *S*-transferase (GST) with either Rpr-TAP (tandem affinity purification tag¹⁶) or Hid-V5 fusions in S2 cells. Wild-type DIAP1 that had been C-terminally fused to GST or amino-terminally tagged with the FLAG

epitope¹⁷ (data not shown) specifically copurified with Rpr (Fig. 2b) and Hid (Fig. 2c). Unexpectedly, Rpr and Hid both copurified with DIAP1 RING finger mutants. However, Hid had a significantly lower binding affinity for DIAP1, compared with the binding of Rpr to DIAP1 (Fig. 2d). Our results indicate that the RING finger of DIAP1 is not necessary for Rpr and Hid binding. Consequently, unlike class I mutations, the failure of class II DIAP1 RING finger mutants to regulate apoptosis induced by Rpr and Hid is not caused by the disruption of DIAP1 binding to Rpr or Hid.

DIAP1 binds to the pro-domain of the initiator caspase Dronc and regulates its activation *in vivo*¹⁸⁻²⁰. We therefore tested whether mutations in either the BIR1 (*th*^{6-3s}), BIR2 (*th*⁴) or the RING domain of DIAP1 (*th*^{21-4s}) affected the binding to Dronc (Fig. 3).

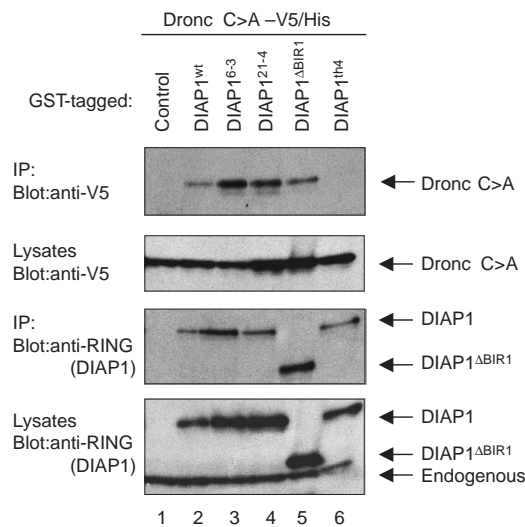


Figure 3 Mutations of the BIR2 domain, but not the RING finger of DIAP1, disrupt binding of Dronc. Copurification of a catalytically inactive Dronc mutant (Dronc C>A) with various DIAP1 mutants from cellular extracts is shown. S2 cells were cotransfected with the indicated constructs, encoding V5-tagged Dronc C>A and GST-tagged wild-type or mutant DIAP1. DIAP1 was purified as described in Fig. 2b and the presence of copurified Dronc C>A was examined by immunoblot analysis using an anti-V5 antibody (top). Expression of V5-tagged Dronc C>A and GST-tagged DIAP1 was confirmed by immunoblotting with the indicated antibodies (second and fourth panel). DIAP1 purification was determined as in Fig. 2b (third panel).

Mutation of the BIR1 domain (class I) or disruption of the DIAP1 RING finger through point mutation or deletion (*th³³⁻¹⁵*; data not shown) had no effect on the ability of DIAP1 to bind to Dronc (Fig. 3). In contrast, *th⁴*, a class III BIR2 mutant of DIAP1 displayed greatly diminished binding to Dronc (Fig. 3), indicating that the BIR2 domain of DIAP1 is required for Dronc binding¹⁹.

We next tested whether DIAP1 RING mutants affect Dronc activation *in vivo* by using transgenic flies that ectopically express Dronc in the developing eye. Expression of Dronc under the control of an eye-specific promoter results in ectopic cell death in the developing retina, causing a 'spotted eye' phenotype¹⁹ (referred to as 'Dronc eye') that is highly sensitive to *diap1* gene dosage¹⁹. Loss of a single allele of *diap1* augments the effect of Dronc so severely that these flies fail to eclose and die trapped in their pupae cases. If the mutant *diap1/th* alleles disrupt the interaction between Dronc and DIAP1, they should enhance the Dronc eye phenotype. To determine the modifier phenotype of the *th* alleles on the Dronc eye phenotype, *pro-dronc^W* transgenic flies were crossed to various *th* mutant flies. Flies carrying the class III *th⁴* allele strongly enhanced the Dronc eye phenotype, indicating that a physical interaction between DIAP1 and Dronc is required to suppress Dronc-mediated cell death (Table 1). Importantly, flies with either an amino acid substitution in the DIAP1 RING finger (*th²¹⁻⁴⁵*) or with a deletion of the entire RING domain (*th³³⁻¹⁵*, data not shown), also had a strongly enhanced Dronc eye phenotype. The Dronc eye phenotype in class II and class III *th* mutant flies was so markedly enhanced that most flies died in their pupae cases with severely deformed eyes (Table 1 and Supplementary Information, Fig. S2). This enhancement of the Dronc eye phenotype is highly reminiscent of the phenotype observed in flies that ectopically express *dronc* and contain only one copy of the *diap1* gene¹⁹. The physical association between DIAP1 and Dronc is necessary, but not sufficient, to regulate Dronc *in vivo* (Table 1). This is evident because DIAP1 RING finger mutants can still bind to Dronc (Fig. 3, compare

lanes 2 and 4), but fail to regulate Dronc activation. These data suggest that after binding, DIAP1 regulates the activity of Dronc through a mechanism that is dependent on the RING finger of DIAP1.

Recent results implicate a function for the RING finger in protein ubiquitination¹¹. We therefore tested whether the RING finger of DIAP1 might be involved in this process. First, we determined the half-life of the DIAP1 protein by treating S2 and Kc cells with either cycloheximide (CHX; Fig. 4a) or *diap1* double-stranded RNA (dsRNAi, Fig. 4b). Both treatments block *de novo* protein synthesis of DIAP1; CHX blocks translation and *diap1* dsRNAi targets *diap1* mRNA for degradation. Thus, we determined that endogenous DIAP1 has a half-life of approximately 30 min (Fig. 4a, compare lanes 5 and 6) and that endogenous DIAP1 protein is intrinsically unstable (Fig. 4a,b). Under the same conditions, tubulin protein was stable and not affected by CHX treatment.

Consistent with the observation that endogenous DIAP1 is unstable, steady-state levels of DIAP1 protein were barely detectable when overexpressed in tissue culture cells (Fig. 4c, lane 1). Compared with wild-type DIAP1 and DIAP1 protein with mutations in either the BIR1 domain or BIR2 domain, DIAP1 protein containing a RING finger mutation was abundantly expressed and readily detectable (Fig. 4c). This implies that the RING finger is a determinant of DIAP1 protein stability. To test whether the ubiquitin-proteasome pathway regulates DIAP1 protein levels, cells expressing wild-type or mutant DIAP1 proteins were treated with lactacystin, a highly specific and irreversible inhibitor of the 20S and 26S proteasome²¹ (Fig. 4c). Lactacystin treatment enhanced the levels of wild-type DIAP1, as well as BIR-mutant DIAP1 proteins (Fig. 4c), suggesting that DIAP1 is degraded by the 26S proteasome. Lactacystin also increased endogenous DIAP1 protein levels (data not shown). The degradation of DIAP1 is dependent on its RING finger, as mutations of this domain, in common with inhibition of the 26S proteasome by lactacystin (Fig. 4c compare lanes 2 and 5), results in enhanced stability of DIAP1.

Proteins with RING finger domains function as E3 ubiquitin protein ligases that promote ubiquitination of both themselves and associated proteins¹¹. We therefore examined whether endogenous DIAP1 is ubiquitinated, and because DIAP1 interacts with Dronc, we determined whether it is also poly-ubiquitinated (Fig. 4d). Kc cells were transiently transfected with a construct expressing haemagglutinin (HA)-tagged ubiquitin. Endogenous DIAP1 and Dronc proteins were immunoprecipitated using anti-DIAP1 or anti-Dronc antibodies, respectively, and immunoblotted for the presence of HA-ubiquitin. Both, endogenous DIAP1 and endogenous Dronc are indeed poly-ubiquitinated *in vivo* (Fig. 4d).

We next tested whether DIAP1 ubiquitinates Dronc *in vivo*. Thus, the indicated proteins were expressed in 293T cells (Fig. 4e). After immunoprecipitation of Dronc, the immunoprecipitated lysates were probed for the presence of ubiquitin with an anti-HA antibody (Fig. 4e). When co-expressed with either wild-type DIAP1 or class I DIAP1 mutants (*th⁶⁻³⁵*), Dronc became heavily poly-ubiquitinated. However, DIAP1 class II RING finger mutants (*th²¹⁻⁴⁵*) failed to promote significant ubiquitination of Dronc. Likewise, class III DIAP1 mutants (*th⁴*) that have impaired binding to Dronc (Fig. 3, compare lanes 2 and 6) also failed to promote Dronc ubiquitination, showing that RING-finger-dependent ubiquitination of Dronc by DIAP1 requires binding. In conclusion, DIAP1-mediated ubiquitination of Dronc depends critically on both their interaction and the presence of a functional DIAP1 RING finger.

We find that in the *Drosophila* eye, mutations affecting the RING finger of endogenous DIAP1 function as loss-of-function mutations that prevent DIAP1 from suppressing Dronc-mediated cell killing. This is evident because both heterozygous *diap1* RING mutant flies (*th²¹⁻⁴⁵/+*) and heterozygous *diap1* flies that carry a deletion in the thread locus (*-/+*) similarly enhance cell killing induced by ectopically expressed Dronc¹⁸⁻²⁰. The eye phenotype is

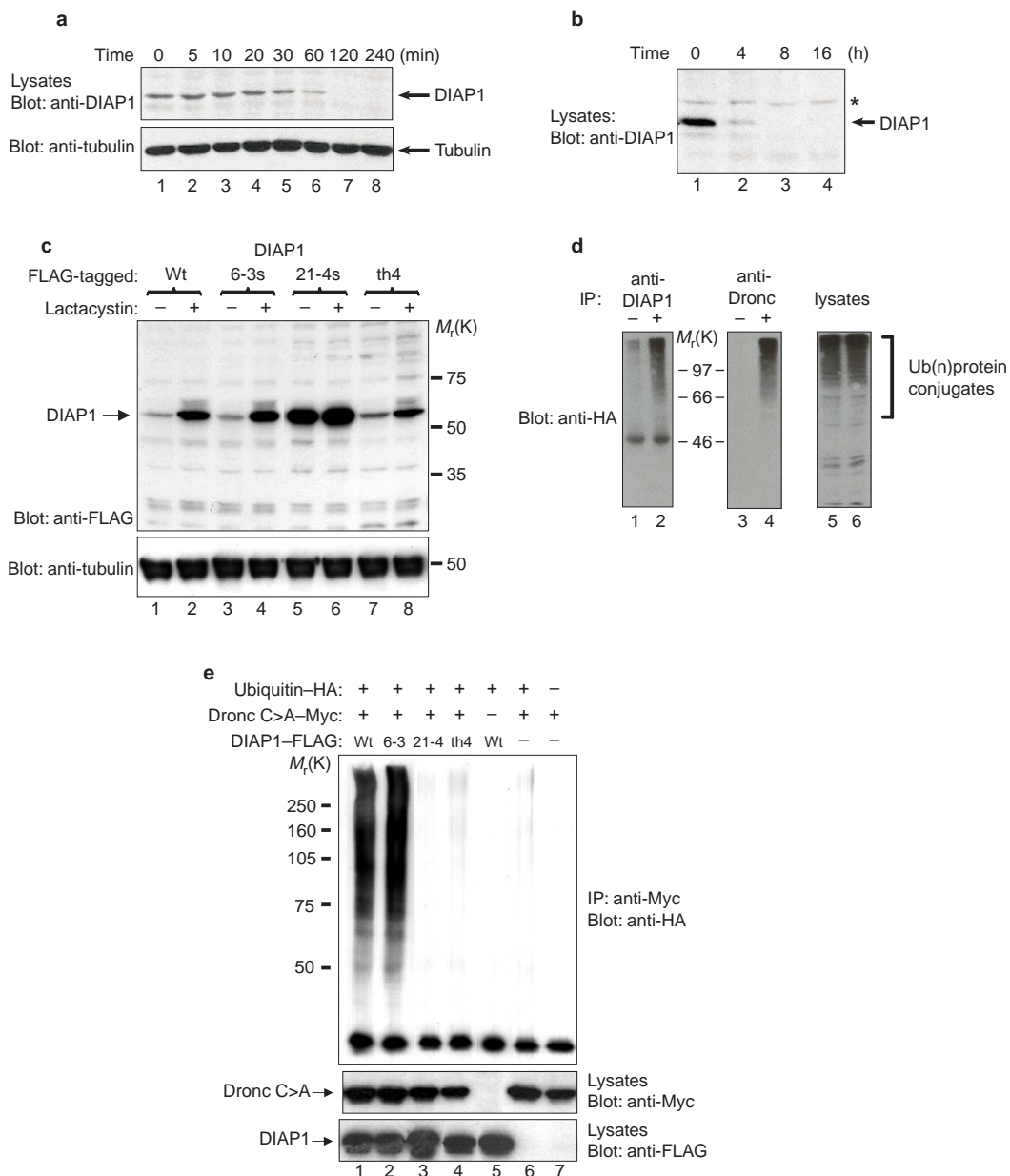


Figure 4 **DIAP1 contains an E3 ubiquitin protein ligase activity that promotes ubiquitination of both itself and Dronc.** **a**, DIAP1 is an unstable protein with a short half-life. S2 cells were treated with CHX and cell extracts were prepared at the times indicated. Expression levels of endogenous DIAP1 protein were detected from whole-cell lysates by immunoblot analysis using an anti-DIAP1 antibody. Tubulin was used as a loading control. **b**, DIAP1 protein levels rapidly diminish in cells that are treated with *diap1* dsRNAi. S2 cells were treated with *diap1* dsRNA and harvested at the indicated times. Expression levels of DIAP1 protein were examined by immunoblot analysis of whole cell lysates using an anti-DIAP1 antibody. The asterisk refers to a non-specific band that functions as a loading control. **c**, DIAP1 degradation by the ubiquitin-proteasome pathway is dependent on its RING finger. 293T cells were transiently transfected with constructs encoding FLAG-tagged wild-type or mutant DIAP1. 24 h after transfection, cells were divided into two dishes and incubated for 18 h with or without lactacystin. Levels of DIAP1 protein were determined by immunoblotting with an anti-FLAG antibody (top). Tubulin was used as a loading control. **d**, Endogenous DIAP1 and Dronc are ubiquitinated *in vivo*. Kc cells

were transiently transfected with a *Drosophila* expression construct encoding HA-tagged ubiquitin. Cell extracts were prepared and denatured by heat treatment before treatment with or without an anti-DIAP1 (first panel) or an anti-Dronc antibody (second panel). The presence of polyubiquitinated forms of DIAP1 (first panel, lane 2) and Dronc (second panel, lane 4) was assessed by immunoblotting with an anti-HA antibody. Expression of HA-ubiquitin was confirmed by immunoblotting of whole-cell lysates with an anti-HA antibody (third panel, lanes 5 and 6). **e**, Dronc ubiquitination is mediated by wild-type DIAP1, but not by DIAP1 mutants that either fail to bind Dronc or carry a RING finger mutation. 293T cells were transiently transfected with the indicated constructs encoding Dronc C>A (Myc-tagged), wild-type or mutant DIAP1 (FLAG-tagged) and HA-tagged ubiquitin. After incubation with lactacystin for 6 h, cell extracts were prepared and immunoprecipitation was performed with an anti-Myc antibody. The presence of polyubiquitinated forms of Dronc C>A was examined by immunoblot analysis with an anti-HA antibody (top). Expression of Myc-tagged Dronc C>A and FLAG-tagged DIAP1 was confirmed by immunoblotting with the indicated antibodies (second and third panel).

Table 1. DIAP1 RING finger mutants enhance the Dronc eye phenotype.

thread alleles	DRONC	Control	Total offspring
Wild type	707	648	1355
class I: 6-3s	1406	948	2354
class II: 21-4s	0	385	1020
class II: <i>th</i> ⁴	176	456	1730

Mutations in the RING finger of DIAP1 or mutations that impair DIAP1 binding to Dronc, fail to regulate Dronc *in vivo*. The ability of different DIAP1 mutants to regulate Dronc *in vivo* was examined by crossing flies ectopically expressing Dronc in the developing eye to either wild-type flies (*yw*) or flies heterozygous for mutations of *diap1* (*th*). Flies with enhanced Dronc eye phenotypes fail to eclose and die trapped in their pupae cases, displaying severely deformed and ruptured eyes (Supplementary Information, Fig. S2). The numbers of emerging offspring of the indicated allelic combinations are given. Individual offspring genotypes are indicated in the Methods. All genetic crosses were performed at 25 °C.

Numbers of adult flies eclosed are shown.

so severe that these flies die encased in their pupae¹⁹ (Table 1). Likewise, DIAP1 proteins with a mutation in the BIR2 domain, which impairs the physical interaction with Dronc, enhance Dronc-mediated killing (Table 1). This indicates that suppression of Dronc-induced cell death by DIAP1 relies on the binding of DIAP1 to Dronc. Importantly, however, the physical interaction between DIAP1 and Dronc is necessary, but not sufficient, for Dronc regulation, as DIAP1 proteins with a mutation affecting the RING finger bind as efficiently to Dronc as wild-type DIAP1, but completely fail to suppress Dronc-mediated killing. Thus, suppression of Dronc-mediated killing by DIAP1 results from a binding-dependent RING finger activity.

A number of studies suggest that proteins with RING finger domains can function as E3 ubiquitin protein ligases¹¹, including some evidence that IAPs might regulate apoptosis by ubiquitinating caspases^{22–24}. We found that both DIAP1 and Dronc are ubiquitinated. This ubiquitination is mediated by an E3 ubiquitin protein ligase activity of the DIAP1 RING finger, because DIAP1 proteins with RING finger mutations are no longer ubiquitinated and fail to ubiquitinate Dronc. The ability of DIAP1 to ubiquitinate Dronc is contingent on their binding, because mutations that disrupt the BIR2–Dronc-binding domain of DIAP1 block ubiquitination of Dronc by DIAP1. These results are consistent with our *in vivo* findings that suppression of Dronc-mediated cell killing by DIAP1 requires both their binding, as well as an intact DIAP1 RING finger domain. Collectively, these data suggest that *in vivo*, DIAP1 suppresses Dronc-induced cell death by binding to Dronc and mediating its ubiquitination by the E3 ubiquitin ligase activity of its RING finger.

Although E3 ubiquitin protein ligases select specific substrates for ubiquitination, the fate of ubiquitinated proteins depends on the type of ubiquitin chain extensions that are made²⁵. We show that DIAP1, in common with many ubiquitinated substrates, is targeted for degradation by the 26S proteasome. In living cells, DIAP1 is a relatively unstable protein that is susceptible to rapid downregulation in response to activation of *rpr*- and UV-mediated apoptosis (P.M., unpublished observations). However, degradation of DIAP1 is strongly inhibited by lactacystin, which specifically inhibits degradation of ubiquitinated proteins by the 26S proteasome²¹. Similarly, disruption of the E3 ubiquitin protein ligase activity of DIAP1 through mutation of the RING finger results in enhanced stability of DIAP1 protein, which is refractory to the effects of lactacystin. Together these data argue that ubiquitination of DIAP1, mediated by its RING finger, targets DIAP1 for degradation

by the 26S proteasome. DIAP1 seems to function as an E3 ubiquitin protein ligase, selecting caspases for ubiquitination. The conjugation of ubiquitin to caspases, such as Dronc, may inactivate them, either by targeting them for degradation or by suppressing caspase activation or activity, for example by blocking their recruitment into apoptosome complexes. Preliminary experiments suggest that ubiquitination of Dronc does not target it for degradation (P.M., unpublished observations).

Our results suggest that IAPs inhibit apoptosis in living cells by ubiquitinating caspases, thereby suppressing their activity. For apoptosis to occur, this IAP-mediated caspase inhibition must be overcome. It seems that in *Drosophila*, Rpr, Grim and Hid induce cell death by binding to DIAP1, thereby liberating caspases^{7,9}. Significantly, Rpr, Grim and Hid all induce cell death through the activation of Dronc^{18–20} (P.M., unpublished observations). According to our model, Rpr, Grim and Hid promote cell death by binding to DIAP1, thereby liberating Dronc from ubiquitination by DIAP1 and allowing activation of the proteolytic caspase cascade, resulting in cell death. Clearly, physical interaction of Rpr and Hid with DIAP1 is required to induce cell death *in vivo*, because mutations of *diap1* that strongly impair its binding to Rpr and Hid severely disrupt Rpr- and Hid-induced cell death⁹. Surprisingly, we found that *diap1* class II RING mutants enhance Rpr-mediated cell death, but suppress Hid-mediated cell death, even though these mutants bind to Rpr and Hid as efficiently as wild-type DIAP1 protein. This may reflect the use of distinct mechanisms by which Rpr and Hid induce cell killing. However, we do not favour this possibility, as we find that both death pathways are affected, indicating that this view may be incorrect. The finding that both Rpr- and Hid-mediated killing are affected indicates that proteins common to both death signalling pathways are affected.

It is possible that the observed differences in Rpr- and Hid-induced killing in the *diap1* RING mutant genetic background reflect a difference in the abilities of Rpr and Hid to physically associate with DIAP1. Hid has a significantly lower binding affinity for DIAP1, compared with the binding of Rpr to DIAP1 (Fig. 2d). These differences in the binding of Rpr and Hid to DIAP1 may explain why Rpr, but not Hid, overcomes increased levels of DIAP1 protein that result from mutation of the RING finger (Fig. 4c, compare lanes 1 and 5). We have shown that mutation of the RING finger results in increased DIAP1 protein stability, as this protein is no longer degraded by the 26S proteasome. According to our model, increased levels of the DIAP1 RING finger mutant protein are sufficient to quench the effects of Hid overexpression, resulting in the observed suppression of Hid-induced cell killing. However, higher levels of the DIAP1 mutant protein are insufficient to overcome the effects of Rpr overexpression, resulting in the observed enhancement of Rpr-mediated cell killing. Rpr-mediated killing is enhanced because DIAP1 RING finger mutants fail to regulate Dronc by ubiquitination. Thus, cells with DIAP1 RING finger mutations are 'sensitized' to undergo cell death because Dronc activation is deregulated.

Our genetic and molecular studies of DIAP1 and the *Drosophila* caspase Dronc indicate that the physical interaction of IAPs with caspases is necessary, but not sufficient, to regulate caspases *in vivo*. We show that the RING finger of DIAP1 is indispensable for the regulation of apoptosis, and that after the binding of DIAP1 to Dronc, the RING finger mediates ubiquitination of Dronc. We propose a model whereby IAPs suppress cell death by ubiquitinating, and thereby inactivating caspases. This inhibition of caspases is dependent on both the binding of IAP and the E3 ubiquitin protein ligase activity of its RING finger. Cell death will be triggered when Rpr-like proteins bind to IAPs, liberating caspases from RING finger-dependent ubiquitination by IAPs.

Note added in proof: Results related to those presented here have been obtained by five other groups and are reported in accompanying papers^{26–30}. □

Methods

Genetic screen and fly stocks

The genetic screen performed to isolate modifiers of *GMR-hid* has been described previously¹⁵. The following mutant and transgenic fly strains were used for the genetic analysis: *GMR-hid*, *GMR-grim* and *GMR-rpr*¹⁵, *th²¹⁻⁴* and *th⁶⁻³* (this study), *th¹* pUAST-*pro-dronc* (8.2a), *GMR-gal4* (816, strong)¹⁹. For the experiment establishing the modifier phenotype of various *th* alleles with respect to *Dronc*, the following genetic crosses were performed and the indicated genotypes and offspring numbers were obtained: *th¹*: F0: 816/SM6;8.2a/TM6 x *yw*¹¹⁸. F1: +/816;+/8.2a (707); *th²¹⁻⁴*/SM6;+/TM6 (648). *th⁶⁻³*: F0: 816/SM6;8.2a/TM6 x *th⁶⁻³*/*th⁶⁻³*. F1: +/816;*th⁶⁻³*/8.2a (1406); *th⁶⁻³*/SM6;+/TM6 (948). *th²¹⁻⁴*: F0: 816/SM6;8.2a/TM6 x *th²¹⁻⁴*/TM3. F1: +/816;*th²¹⁻⁴*/8.2a (0); +/816;TM3/8.2a (432); +/TM3;SM6/TM3 (203); *th²¹⁻⁴*/SM6;+/TM6 (385). *th⁴*: F0: 816/SM6;8.2a/TM6 x *th⁴*/TM3. F1: +/816;*th⁴*/8.2a (176); +/816;TM3/8.2a (793);+/TM3,SM6/TM3 (305); *th⁴*/SM6;+/TM6 (456). SM6 and TM6 are on a compound chromosome. All genetic crosses were performed at 25 °C.

Electron microscopy

Electron microscopy was performed as previously described⁸.

Generation of expression constructs and molecular analysis of the mutants

dronc, *rpr* and *hid*, and the various *diap1* fragments, were amplified by PCR using Expand High Fidelity (Roche, Germany) and cloned as follows. *diap1* and its various mutants were cloned into the *Drosophila* vector pMTIZ-GST. The cDNAs encoding the *dronc* C318A mutant and *hid* were cloned into the pMT vector (Invitrogen, The Netherlands) in-frame with the V5 tag. *rpr* constructs were cloned into the pMTIZ-TAP tag vector. All the above mentioned tags were expressed at the C terminus of the proteins. Wild-type *diap1*, *th⁶⁻³*, *th²¹⁻⁴* and *th⁴* were amplified by PCR and cloned into the mammalian expression vector pcDNA3.1. All constructs were verified by DNA sequencing. The mammalian *dronc* C>A expression vector was previously described¹⁹. The molecular nature of the *th* mutant flies was determined as described previously⁹. Mutant *diap1* cDNAs were amplified by PCR from mutant flies and cloned into pIE1-3 (Novagen, The Netherlands) as described previously⁹.

Cell culture, dsRNAi, transfections and apoptosis assay

293T cells were cultured as described previously¹⁹. The *Drosophila* cell lines S2 and Kc were cultured in *Drosophila* Schneider medium (Gibco-BRL, UK) in the presence of 10% foetal calf serum. 293T cells were transfected with FuGene6 (Roche), Rat1 cells with Superfect (Gibco-BRL) and the *Drosophila* cell lines were either transfected using Cellfectin (Gibco-BRL) or calcium phosphate (Clontech, Palo Alto, CA) according to the manufacturer's instructions. Apoptosis assays were performed as previously described¹⁵. dsRNAi experiments were performed in accordance with protocols published online (<http://dixonlab.biochem.med.umich.edu/protocols/RNAiExperiments.html>). The first 700 bp of the *diap1* coding sequence was used to knock down *diap1* levels.

Protein extracts and immunoprecipitation/copurification assays

Drosophila S2 cells plated in 6-well plates were transfected with the following plasmids: pMTIZ-GST (control), pMTIZ-*diap1*-wt-GST, pMTIZ-*diap1*-*th⁶⁻³*-GST, pMTIZ-*diap1*-*th²¹⁻⁴*-GST, pMTIZ-*diap1*-ΔBIR1-GST, pMTIZ-*diap1*-*th⁴*-GST, pMT-*dronc*-C318A-V5/His, pMTIZ-*rpr*-TAP and pMT-*hid*-V5/His. The cells were induced overnight with copper sulphate 24 h after transfection and lysed in lysis buffer [50 mM Tris-HCl at pH 8.0, 150 mM sodium chloride, 1 mM EDTA, 10% Glycerol, 1% Triton-X100 and Complete protease inhibitor cocktail (Roche)]. The lysates were centrifuged at 20,000g for 15 min at 4 °C and the supernatants were incubated with glutathione beads for 1 h at 4 °C. The beads were washed five times with washing buffer (10 mM Tris-HCl at pH 8.0, 150 mM sodium chloride and 0.1% Triton-X100) and GST-tagged proteins were eluted with 10 mM reduced glutathione (GSH). Immunoprecipitation assays using lysates from transiently transfected 293T cells were conducted as previously described¹⁹.

Treatments with proteasome inhibitor and cycloheximide

The proteasome inhibitor lactacystin (Calbiochem, UK) was used at of 8 μM and cells were incubated for up to 6 h in the presence of lactacystin. Briefly, 293T or Rat1 cells were transiently transfected with various *diap1* expression constructs. 24 h after transfection, cells from each tissue culture dish were split and divided into two dishes to avoid variations in transfection efficiencies. After a further incuba-

tion of 18 h, each dish was treated for 6 h, either with dimethylsulphoxide or lactacystin. For the experiment determining DIAP1 protein half-life, S2 cells were treated with 50 μg ml⁻¹ CHX for the times indicated.

Generation of anti-DIAP1 RING antibodies

A fragment of *diap1* cDNA encoding the 97 C-terminal amino acids of DIAP1 was amplified by PCR and cloned into the bacterial expression vector pGEX-6P1 (Amersham Pharmacia Biotech, UK). The GST-DIAP1-RING-fusion protein was purified from bacteria and the DIAP1 RING portion of the GST-fusion protein was cleaved using the precision protease (Amersham Pharmacia Biotech). Anti-DIAP1 RING antibodies were generated by inoculating guinea pigs with purified DIAP1 RING protein.

RECEIVED 30 JANUARY 2002; REVISED 5 MARCH 2002; ACCEPTED 10 APRIL 2002; PUBLISHED 14 MAY 2002.

1. Meier, P., Finch, A. & Evan, G. *Nature* **407**, 796–801 (2000).
2. Thornberry, N. A. & Lazebnik, Y. *Science* **281**, 1312–1316 (1998).
3. Alnemri, E. S. J. *Cell. Biochem.* **64**, 33–42 (1997).
4. Hengartner, M. O. *Nature* **407**, 770–776 (2000).
5. Uren, A. G., Coulson, E. J. & Vaux, D. L. *Trends Biochem. Sci.* **23**, 159–162 (1998).
6. Deveraux, Q. L. & Reed, J. C. *Genes Dev.* **13**, 239–252 (1999).
7. Wang, S. L., Hawkins, C. J., Yoo, S. J., Muller, H. A. & Hay, B. A. *Cell* **98**, 453–463 (1999).
8. Lisi, S., Mazzon, I. & White, K. *Genetics* **154**, 669–678 (2000).
9. Goyal, L., McCall, K., Agapite, J., Hartwig, E. & Steller, H. *EMBO J.* **19**, 589–597 (2000).
10. Goyal, L. *Cell* **104**, 805–808 (2001).
11. Joazeiro, C. A. & Weissman, A. M. *Cell* **102**, 549–552 (2000).
12. Grether, M. E., Abrams, J. M., Agapite, J., White, K. & Steller, H. *Genes Dev.* **9**, 1694–1708 (1995).
13. Hay, B. A., Wassarman, D. A. & Rubin, G. M. *Cell* **83**, 1253–1262 (1995).
14. White, K., Tahaoglu, E. & Steller, H. *Science* **271**, 805–807 (1996).
15. Bergmann, A., Agapite, J., McCall, K. & Steller, H. *Cell* **95**, 331–341 (1998).
16. Rigaut, G. *et al. Nature Biotechnol.* **17**, 1030–1032 (1999).
17. Vucic, D., Kaiser, W. J. & Miller, L. K. *Mol. Cell. Biol.* **18**, 3300–3309 (1998).
18. Hawkins, C. J. *et al. J. Biol. Chem.* **275**, 27084–27093 (2000).
19. Meier, P., Silke, J., Leever, S. J. & Evan, G. I. *EMBO J.* **19**, 598–611 (2000).
20. Quinn, L. M. *et al. J. Biol. Chem.* **275**, 40416–40424 (2000).
21. Fenteany, G. & Schreiber, S. L. *J. Biol. Chem.* **273**, 8545–8548 (1998).
22. Yang, Y., Fang, S., Jensen, J. P., Weissman, A. M. & Ashwell, J. D. *Science* **288**, 874–877 (2000).
23. Suzuki, Y., Nakabayashi, Y. & Takahashi, R. *Proc. Natl. Acad. Sci. USA* **98**, 8662–8667 (2001).
24. Huang, H. *et al. J. Biol. Chem.* **275**, 26661–26664 (2000).
25. Pickart, C. M. *Mol. Cell* **8**, 499–504 (2001).
26. Holley *et al. Nature Cell Biol.* DOI: 10.1038/ncb798.
27. Ryoo *et al. Nature Cell Biol.* DOI: 10.1038/ncb795.
28. Wing *et al. Nature Cell Biol.* DOI: 10.1038/ncb800.
29. Hays *et al. Nature Cell Biol.* DOI: 10.1038/ncb794.
30. Yoo *et al. Nature Cell Biol.* DOI: 10.1038/ncb793.

ACKNOWLEDGEMENTS

We wish to thank K. White for the generous gift of anti-DIAP1 antibody, D. Bohmann for the HA-ubiquitin construct and B. Seraphin for the TAP-construct. We thank T. Tenev for technical advice and graphical support and members of the laboratory for discussions. Furthermore, we thank members of the Evan and Downward laboratories for helpful discussions and support. We also thank S. Schneider for critical reading of the manuscript. We apologize to the scientists whose work we could not cite because of space limitations. H.S. is an investigator of the Howard Hughes Medical Institute. Part of this work was supported by National Institutes of Health grant RO1GM60124. Correspondence and requests for materials should be addressed to P.M. Supplementary information is available on *Nature Cell Biology's* website (<http://cellbio.nature.com>).

COMPETING FINANCIAL INTERESTS

The authors declare that they have no competing financial interests.